Journal of Alloys and Compounds 505 (2010) 675–679

Contents lists available at ScienceDirect

Journal of Alloys and Compounds

journal homepage: www.elsevier.com/locate/jallcom

Microstructure and oxidation resistance of magnetron-sputtered nanocrystalline NiCoCrAlY coatings on nickel-based superalloy

Zhiming Li, Shiqiang Qian*, Wei Wang, Jihua Liu

College of Material Engineering, Shanghai University of Engineering Science, Shanghai 201620, China

ARTICLE INFO

Article history:
Received 14 May 2010
Accepted 16 June 2010
Available online 30 June 2010

Keywords:
NiCoCrAlY coating
Magnetron sputtering
Microstructure
High temperature oxidation resistance
Nickel-based superalloy

ABSTRACT

Nanocrystalline NiCoCrAlY coatings on GH3128 nickel-based superalloy were produced using DC magnetron sputter deposition with a composite target. The microstructure and morphology of coatings were investigated using X-ray diffraction (XRD), scanning electron microscope (SEM), energy dispersive X-ray analysis (EDAX) and atomic force microscopy (AFM). Isothermal-oxidation tests were performed at 1100 °C in air for 24 h. The results show that the magnetron-sputtered NiCoCrAlY coating possesses a polycrystalline austenitic structure (FCC) with lattice constant 0.359821 nm. The (2 2 0) is the preferred growth direction of the NiCoCrAlY coating and the coating grain size is about 70 nm. The isothermal-oxidation test results exhibit that the oxidation kinetics of substrate and coating specimens all basically follow the parabolic rate law. However, the weight gain rate constant of coating is only about one-fifth of that of substrate. The weight gain of NiCoCrAlY coated specimen is only 48.16% of the superalloy substrate specimen after the isothermal-oxidation test. The above results reveal that the magnetron-sputtered nanocrystalline NiCoCrAlY coating is quite effective to increase the high temperature oxidation resistance of GH3128 superalloy.

1. Introduction

Operating temperatures of jet turbine engines are now reaching limits posed by the melting temperatures (T_m) of nickel-based superalloys [1]. Thermal barrier coatings (TBCs) are needed to protect these superalloy components. TBCs can insulate turbine engine components from the hot gas stream as well as improve the durability and energy efficiency of turbine engines [2]. The metal bond coat and ceramic topcoat are the main parts of TBCs. They are now being seriously examined by academic and industrial groups.

The alloy bond coat, which acts as an important part of TBCs, oxidizes to form a passive oxide layer and also provides adhesion between the ceramic topcoat and the substrate [3]. MCrAlY coat (M = Ni and/or Co) is one of the mostly commonly used bond coat in TBCs [4]. The concentrations of alloying elements in this bond coat have great effects on the performance of TBC systems [4,5]. Stecura [5] reported that without yttrium in the bond coat, the TBC failed very rapidly. His studies also showed that increasing concentrations of chromium and aluminum in the NiCrAlY bond coat increased the total TBC lifetimes. Oxidation behaviour of this bond coats was a hot point and front line gambit in recent years [6–9]. In the oxidation process, the diffusion of the superalloy substrate element Ti to the surface of the bond coat would lead to spallation of the protective oxide layer [10]. The formation of a continuous thermally grown oxide (TGO) layer protects the coating from further oxidation and avoids the formation of mixed oxide protrusion to a certain extent [11]. Di Ferdinando et al. [12] performed a comparative study on isothermal-oxidation resistance of air plasma sprayed (APS), vacuum plasma sprayed (VPS) and high velocity oxygen fuel sprayed (HVOF) CoNiCrAlY bond coats. It was found that HVOF technique provided bond coats with higher oxidation resistance compared to APS and VPS. Similarly, Yuan et al. [13] reported that the isothermal-oxidation rate at 1100 °C of the TBCs with the HVOF bond coat was two times lower than that of the TBCs with the detonation-sprayed bond coat. In addition, mechanical property of these coatings is also an important research subject. The residual stress is compressive in the plasma sprayed NiCoCrAlY bond coat, and the ductile to brittle transition temperature (DBTT) of this bond coat is about 650 °C [14]. Almost all of these studies were realized by spraying or electron beam physical vapor deposition (EB-PVD). However, few studies have been done to prepare this bond coat using magnetron sputtering, which is an excellent technique to produce high-quality films and coatings [15].

In the present investigation, NiCoCrAlY coating on GH3128 nickel-based superalloy was prepared by magnetron sputtering to improve the high temperature oxidation resistance of superalloy. Certainly this alloy coat would serve as the bond coat in the later studies on thermal barrier coating system. The structure, morphol-

* Corresponding author. Tel.: +86 21 67791203; fax: +86 21 67791201.
E-mail addresses: li-zhiming@hotmail.com (Z. Li), qshiqiang@163.com (S. Qian).

0925-8388/$ – see front matter © 2010 Elsevier B.V. All rights reserved.
doi:10.1016/j.jallcom.2010.06.112

Table 1
Chemical analysis of the substrate (GH3128 superalloy).

Material	Elements/wt.%										
	Cr	W	Mo	Al	Ti	Fe	C	Ce	Zr	B	Ni
GH3128 superalloy	20.55	8.70	8.26	0.80	0.40	0.60	0.04	0.05	0.08	0.05	Bal.

ogy, composition and oxidation resistance of magnetron-sputtered nanocrystalline NiCoCrAlY coating were investigated.

2. Experimental

2.1. Deposition and characterization of samples

The substrate material used in this study was a nickel-based superalloy GH3128 (see Table 1), which is mostly employed for manufacturing flame tube, tailpipe chamber and other high-temperature components in gas turbines. DC magnetron sputter deposition was used to produce the alloy coating. The NiCoCrAlY alloy target had a diameter of 60 mm and a thickness of 3 mm. The NiCoCrAlY coatings were deposited on square-shaped GH3128 superalloy coupons of 15 mm × 15 mm × 2.5 mm, which were mechanically polished to the surface roughness of 12 nm and thoroughly cleaned before the coating deposition. The operating conditions for the DC magnetron sputtering system were set at a base pressure of 3.4×10^{-6} Torr, working pressure of 7.5 mTorr, argon (Ar) flow of 5.4 sccm, target to substrate distance of 80 mm, substrate temperature of 25 °C, sputtering time of 45 min, respectively, and sputtering powers of 100 W.

The X'Pert Pro X-ray diffractometer (XRD) with Cu-Kα radiation was used to investigate the structure of samples. A HITACHI S-3400N scanning electron microscope (SEM) with energy dispersive X-ray detector (EDX) system was used to measure the coating composition. A NanoScope IIIa atomic force microscope (AFM) was used in tapping mode and ambient conditions to study the surface morphology of the coatings. The SEM was also used to investigate the cross-sectional morphology of the coating–substrate system.

2.2. Isothermal-oxidation testing

For comparison, the uncoated samples were also oxidation tested, and mechanically polished to the surface roughness of 12 nm before the oxidation tests. All samples were ultrasonically cleaned with acetone. A perpendicular tube furnace with a temperature accuracy of ±0.5 °C in the hot zone was used. Samples were put into crucible and the crucible was placed into the hot zone of the furnace. The mass-change of samples during the isothermal-oxidation tests was real-time detected by using an electronic analytical balance and a computer. Isothermal-oxidation tests of the coated and uncoated sample were performed at 1100 °C in ambient atmosphere for 24 h, and the data-collection interval in this study was 12 s. X-ray diffraction (XRD) with Cu-Kα radiation was used to study the phase composition of the oxidation products on the surface of samples after oxidation tested.

3. Results and discussion

3.1. Microstructural characterization

The XRD patterns of superalloy substrate (a), NiCoCrAlY coating (b) and sputtering target (c) are presented in Fig. 1. It seems

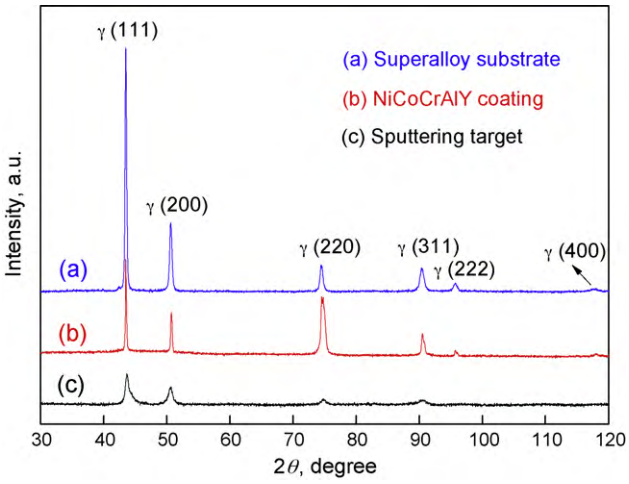

Fig. 1. XRD patterns of NiCoCrAlY coating, superalloy substrate and sputtering target.

that the coating, substrate and target predominantly have a same polycrystalline γ austenitic structure (FCC). Furthermore, detail information about the structure of substrate, coating and target were distinguishing according to further analyses and calculations. Intensity of the main diffraction peaks and lattice constant of coating, substrate and target are listed in Table 2. The diffraction peaks of superalloy substrate and NiCoCrAlY coating are sharp and strong. It is indicative of the well crystallinity of both the superalloy and NiCoCrAlY coating. However, the diffraction intensity of sputtering target is relatively low, which indicates that the sputtering target was crystallized imperfectly. The lattice constant of standard γ-Ni phase is 0.352380 nm according to the data of standard PDF card 00-004-0850. However, the lattice constant of superalloy substrate, NiCoCrAlY coating and sputtering target possessed an increase of 0.007859, 0.007441, and 0.007598 nm, respectively, due to the solutionizing of alloying elements. It also can be seen that the (2 2 0) is the preferred growth direction of the NiCoCrAlY coating. According to Scherrer equation, the average crystal size of the sputtered NiCoCrAlY coating was about 70 nm.

The superficial SEM image and EDAX analysis of the NiCoCrAlY coating are shown in Fig. 2. The coating produced with the NiCoCrAlY composite target contained 48.80 wt.% Ni, 23.06 wt.% Co, 19.81 wt.% Cr and 8.33 wt.% Al. However, the yttrium content was too low to be detected by the energy dispersive X-ray detector.

Fig. 3 shows the AFM image of the coating surface. The NiCoCrAlY coating obtained from the DC magnetron sputter deposition was observed to be uniform and to present a fine-grain coating

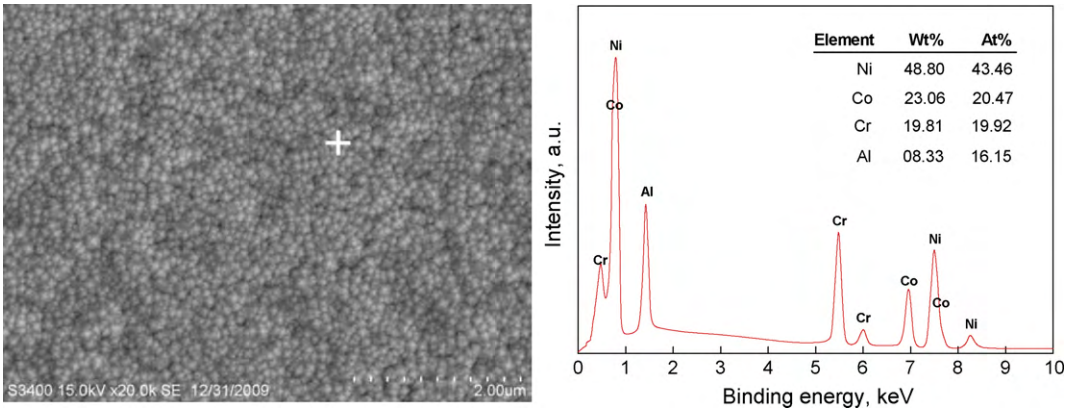

Fig. 2. Superficial SEM images and EDAX analysis of the NiCoCrAlY coating.

Table 2
Intensity of the main diffraction peaks and lattice constant of coating, substrate and target.

Description	$I_{(111)}$/counts	$I_{(200)}$/counts	$I_{(220)}$/counts	$I_{(311)}$/counts	$I_{(111)}/I_{(200)}/I_{(220)}/I_{(311)}$	a/nm
Substrate	15,234	4019	1693	1420	100/26.4/11.1/9.3	0.360239
Coating	6447	2659	3924	1529	100/41.2/60.9/23.7	0.359821
Target	1638	831	305	211	100/49.7/18.6/14.9	0.359978
Standard γ	–	–	–	–	100/42/21/20	0.352380

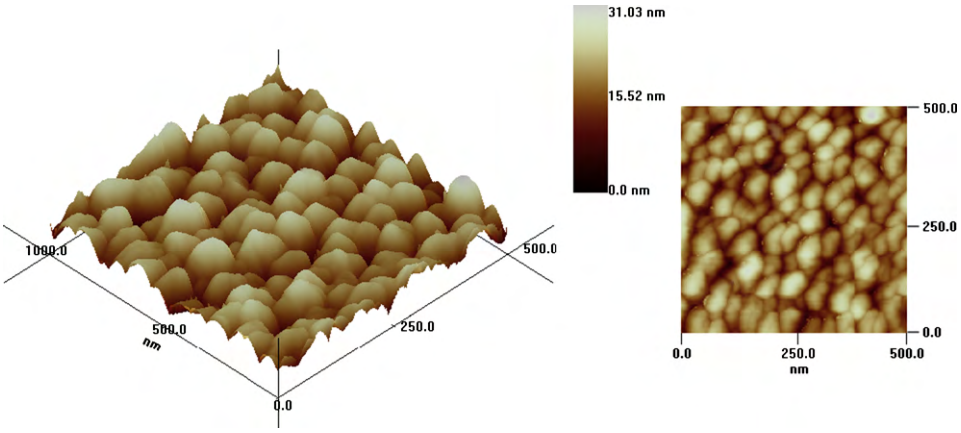

Fig. 3. Three-dimensional and two-dimensional AFM images of the NiCoCrAlY coating surface.

microstructure, as shown in the AFM and SEM images. The coating grain size was estimated to be ~70 nm according to the linear-intercept measurement, which was substantially consistent with the XRD analysis result.

Fig. 4 presents the cross-sectional SEM images of the coating–substrate system. It can be seen that a very dense and homogeneous coating microstructure was produced. The thickness of as-deposited NiCoCrAlY coating was about 3.5 μm. According to calculation, the deposition rate of NiCoCrAlY coating under the condition of this study was about 1.3 nm per second.

3.2. High temperature oxidation resistance and analysis

Fig. 5 illustrates the isothermal-oxidation kinetics of coated and uncoated specimens at 1100 °C. The rings and solid lines represent mass gain data points and quadratic fitting curves of these data points, respectively. Although the data points are fluctuant due to the testing instability, the mass gain of both the superalloy and NiCoCrAlY coating has a growing tendency on the whole. Obviously the NiCoCrAlY coated specimen had lower mass gain than the uncoated superalloy substrate during 24 h (86,400 s) of isothermal-oxidation process.

The related oxidation reactions of the coated and uncoated specimens are as follows:

$$2Co(s) + O_2(g) = 2CoO(s) \quad (1)$$

$$2Ni(s) + O_2(g) = 2NiO(s) \quad (2)$$

$$4Cr(s) + 3O_2(g) = 2Cr_2O_3(s) \quad (3)$$

$$4Al(s) + 3O_2(g) = 2Al_2O_3(s) \quad (4)$$

$$4Y(s) + 3O_2(g) = 2Y_2O_3(s) \quad (5)$$

$$CoO(s) + Cr_2O_3(s) = CoCr_2O_4(s) \quad (6)$$

$$NiO(s) + Cr_2O_3(s)\,NiCr_2O_4(s) \quad (7)$$

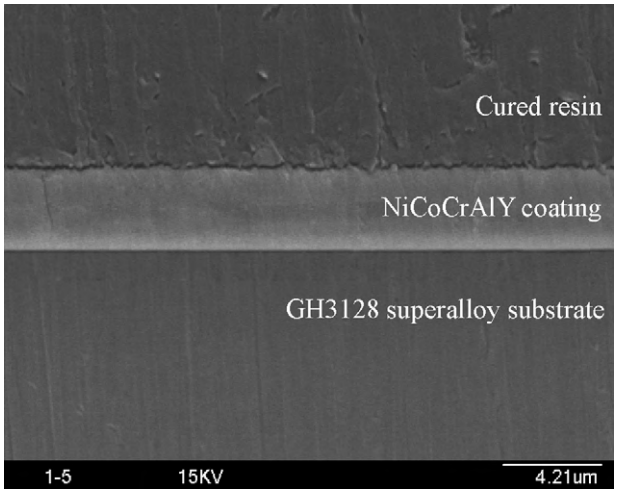

Fig. 4. Cross-sectional SEM images of the coating–substrate system.

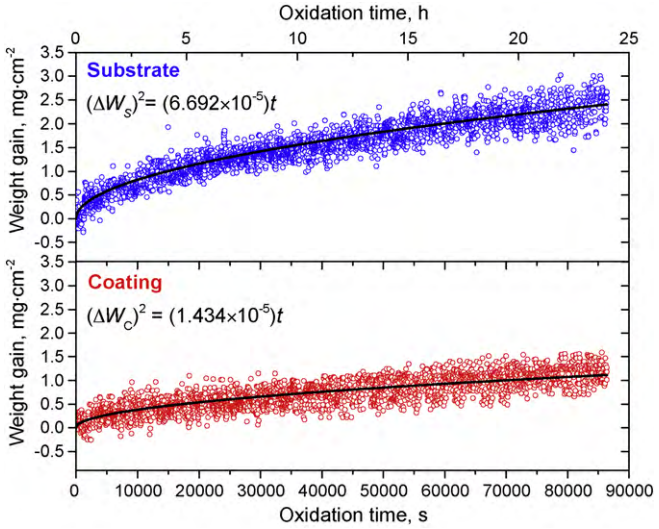

Fig. 5. Isothermal-oxidation kinetics of coated and uncoated specimens at 1100 °C.

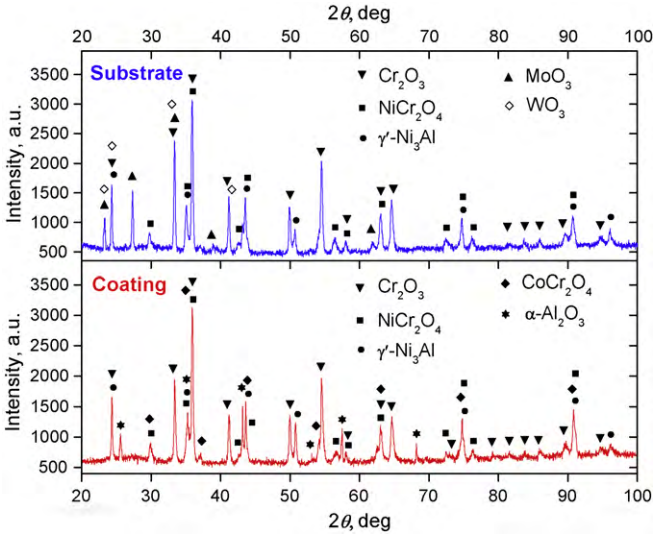

Fig. 6. XRD patterns of isothermal-oxidation tested specimens.

$$2Mo(s) + 3O_2(g) = 2MoO_3(s) \quad (8)$$

$$2W(s) + 3O_2(g) = 2WO_3(s) \quad (9)$$

where reactions of Eqs. (1)–(5) and (8) and (9) are zero order irreversible reaction. Eqs. (1)–(7) are the oxidation reaction in the NiCoCrAlY coating. Reactions of Eqs. (1)–(5) result in weight gain of coating specimens, and they are treated as a whole weight gain (ΔW_C) in the coating. Meanwhile, Eqs. (2)–(4) and (6)–(9), as oxidation reactions of the superalloy substrate, are also treated as a whole reaction, which cause the weight gain (ΔW_S) in the substrate.

From the data points obtained by oxidation testing (shown in Fig. 5), the oxidation kinetics of substrate and coating specimens are all basically in accord with the parabolic rate law. Thus, the weight gain in the coating and substrate specimens can be expressed as

$$(\Delta W_C)^2 = k_C t \quad (10)$$

$$(\Delta W_S)^2 = k_S t \quad (11)$$

where k_C and k_S are the weight gain rate constant of coating and substrate, respectively. The weight gain rate constant depends on oxidation temperature, structure and composition of the materials. Here the oxidation time is in seconds, and the unit for the weight gain is milligram per square centimeter. Then, parabola function was used to fit the data points, and the fitting results are as follows:

$$k_C = 1.434 \times 10^{-5}\ mg^2\ cm^{-4}\ s^{-1} \quad (12)$$

$$k_S = 6.692 \times 10^{-5}\ mg^2\ cm^{-4}\ s^{-1} \quad (13)$$

The results show that k_C is only about one-fifth of k_S, which means that the oxidation rate of NiCoCrAlY coating is much slower than that of the uncoated GH3128 superalloy. Evidently the magnetron-sputtered nanocrystalline NiCoCrAlY coating can effectively protect the superalloy substrate from oxidation at high temperature.

After the oxidation testing, the mass gain of substrate specimen was 2.45 mg/cm^2, while for the NiCoCrAlY coated specimen was 1.18 mg/cm^2, only 48.16% of the substrate specimen. Therefore, it also evidence that the magnetron-sputtered nanocrystalline NiCoCrAlY coating has a better high temperature oxidation resistance than the uncoated GH3128 superalloy.

Fig. 6 gives the XRD patterns of the specimens after isothermal-oxidation testing at 1100 °C for 24 h. It can be seen that the common phase compositions of uncoated substrate specimen and NiCoCrAlY coating specimen after oxidation were Cr_2O_3, $NiCr_2O_4$, and γ′-Ni_3Al. The mixed oxides, which were in the form of Cr_2O_3, $NiCr_2O_4$, played a detrimental role in causing crack nucleation and growth, and reducing the life of the coating system in air [16]. According to the previous EDAX analysis, the content of Al in substrate specimen was only 0.80 wt.%. Then it can be supposed that Ni_3Al phase was the main existence form of Al in substrate specimen after oxidation testing. The precipitation of Ni_3Al phase probably led to overall strengthening of the superalloy substrate [14]. It was extremely important to note that the oxidation products of substrate specimen contained some MoO_3 and WO_3, while they were not existed in the coated specimen. It means that with no protection from NiCoCrAlY coating, the molybdenum and wolfram on the surface of the substrate specimen were oxidized. As the MoO_3 and WO_3 are volatile at high temperature, the detected oxide generated during the cool down operation. Spinel $CoCr_2O_4$ was found in coated specimen after oxidation testing due to the presence of cobalt in coating. It was evident that α-Al_2O_3 existed in the surface of the coating specimen after the oxidation testing and it up to a considerable amount. However, no α-Al_2O_3 was detected in substrate specimen after oxidation; it should be due to its extremely low content.

The magnetron-sputtered nanocrystalline NiCoCrAlY coatings possess much higher oxidation resistance than the uncoated superalloy as the above analysis. Certainly the α-Al_2O_3 formed at the early stages of oxidation played an important role in the oxidation resistance of this coating. The α-Al_2O_3 layer was stable and can effectively prevent or relieve the proliferation of oxygen within the specimens [17]. As in TBC system, the selective oxidation of Al in the NiCoCrAlY bond coat and a Ni_3Al film on the surface of this bond coat would lead to an Al_2O_3 layer between the NiCoCrAlY bond coat and the transition layer [18]. The Al_2O_3 layer is propitious to the adherence of the ceramic topcoat onto the metallic bond coat in TBC system. However, if the thickness of the Al_2O_3 layer is greater than 3 μm, the ceramic topcoat would spall from the metallic bond coat; hence the TBC system is failed [19].

Furthermore, grain size of coatings has important effects on selective oxidation behaviour of the alloys [20]. For this study, the nanostructured characteristic of the magnetron-sputtered NiCoCrAlY coating also played a certain role in the oxidation resistance. We believe that increased aluminum diffusion through the grain boundaries of nanostructured NiCoCrAlY coating would favor the nucleation of the Al_2O_3 layer. Once the stable alumina layer is formed, it reduces the rate of oxidation in the alloy coating. Nevertheless, future study is necessary to disclosure the accurate distribution and amount of oxides in the oxidated nanocrystalline magnetron-sputtered NiCoCrAlY coating, so as to completely understand the microscopic oxidation mechanism of this coating.

4. Conclusions

The structure and morphology of magnetron-sputtered NiCoCrAlY coating were characterized, the weight gain of specimens in isothermal-oxidation testing as well as the phase composition of oxidation products were studied; the following conclusions can be drawn:

(1) The magnetron-sputtered NiCoCrAlY coating, GH3128 superalloy substrate and sputtering target predominantly possess same polycrystalline γ austenitic structure (FCC). Their lattice constants are about 0.359821, 0.360239, and 0.359978 nm, respectively, larger than the standard γ-Ni phase (0.352380 nm) due to the solutionizing of alloying elements. The (2 2 0) is the preferred growth direction of the NiCoCrAlY coating and the coating grain size is about 70 nm.
(2) When NiCoCrAlY coating was magnetron sputtered onto the GH3128 superalloy, great effects of nanocrystalline NiCoCrAlY

coating on the high temperature oxidation resistance of the specimen were found. The oxidation kinetics of substrate and coating specimens all basically follow the parabolic rate law. However, the weight gain rate constant of coating is only about one-fifth of that of substrate. The weight gain of NiCoCrAlY coated specimen is only 48.16% of the GH3128 superalloy substrate specimen after 24 h of isothermal-oxidation at 1100 °C in ambient atmosphere. In addition to nickel-chromium oxides, some MoO_3 and WO_3 appear in the oxidation products of substrate specimen. The α-Al_2O_3 layer formed at the early stages of oxidation play a major role in the oxidation resistance of NiCoCrAlY coating.

Acknowledgements

The authors gratefully acknowledge the financial supports from Special Foundation of the Shanghai Education Commission for Nano-Materials Research (0852nm01400) and Shanghai Leading Academic Discipline Project (J51402).

References

[1] J.H. Perepezko, Science 326 (2009) 1068–1069.
[2] N.P. Padture, M. Gell, E.H. Jordan, Science 296 (2002) 280–284.
[3] R. Krishnamurthy, D.J. Srolovitz, Mater. Sci. Eng. A 509 (2009) 46–56.
[4] T. Patterson, A. Leon, B. Jayaraj, J. Liu, Y.H. Sohn, Surf. Coat. Technol. 203 (2008) 437–441.
[5] S. Stecura, Thin Solid Films 73 (1980) 481–489.
[6] F. Cao, B. Tryon, C.J. Torbet, T.M. Pollock, Acta Mater. 57 (2009) 3885–3894.
[7] T. Xu, S. Faulhaber, C. Mercer, M. Maloney, A. Evans, Acta Mater. 52 (2004) 1439–1450.
[8] B.G. Mendis, B. Tryon, T.M. Pollock, K.J. Hemker, Surf. Coat. Technol. 201 (2006) 3918–3925.
[9] W.J. Quadakkers, V. Shemet, D. Sebold, R. Anton, E. Wessel, L. Singheiser, Surf. Coat. Technol. 199 (2005) 77–82.
[10] A. Hesnawi, H. Li, Z. Zhou, S. Gong, H. Xu, Vacuum 81 (2007) 947–952.
[11] L. Ajdelsztajn, J.A. Picas, G.E. Kim, F.L. Bastian, J. Schoenung, V. Provenzano, Mater. Sci. Eng. A 338 (2002) 33–43.
[12] M. Di Ferdinando, A. Fossati, A. Lavacchi, U. Bardi, F. Borgioli, C. Borri, C. Giolli, A. Scrivani, Surf. Coat. Technol. 204 (2010) 2499–2503.
[13] F.H. Yuan, Z.X. Chen, Z.W. Huang, Z.G. Wang, S.J. Zhu, Corros. Sci. 50 (2008) 1608–1617.
[14] A.K. Ray, N. Roy, A. Kar, A.K. Ray, S.C. Bose, G. Das, J.K. Sahu, D.K. Das, B. Venkataraman, S.V. Joshi, Mater. Sci. Eng. A 505 (2009) 96–104.
[15] S. Ulrich, J. Ye, M. Stüber, C. Ziebert, Thin Solid Films 518 (2009) 1455–1458.
[16] W.R. Chen, X. Wu, B.R. Marple, P.C. Patnaik, Surf. Coat. Technol. 197 (2005) 109–115.
[17] X. Yang, X. Peng, F. Wang, Corros. Sci. 50 (2008) 3227–3232.
[18] H. Guo, S. Gong, C. Zhou, H. Xu, Surf. Coat. Technol. 148 (2001) 110–116.
[19] B. Goswami, B. Ravi Kumar, S. Tarafder, G. Krishna, P Karuna Purnapu Rupa, S.B. Kumar, A.K. Ray, High Temp. Mater. Process. 26 (2007) 209–219.
[20] Z. Liu, W. Gao, K.L. Dahm, F. Wang, Acta Mater. 46 (1998) 1691–1700.